

DOI: 10.1070/QEL16036

Suppression of the contribution of short trajectories into above-threshold ionisation spectra by a two-colour laser field

N.V. Vvedenskii, A.N. Zheltukhin, A.A. Silaev, D.V. Knyazeva,
N.L. Manakov, A.V. Flegel, M.V. Frolov

Abstract. **We have studied spectra of above-threshold ionisation of atoms by a two-colour laser field with collinear linearly polarised components. We have found a sharp (gap-like) dependence of the length of the high-energy plateau in above-threshold ionisation spectra on the relative phase of the two-colour field at comparable intensities of the field components. Using the quasi-classical analysis we have shown that this effect results from the suppression of partial above-threshold ionisation amplitudes, associated with closed classical trajectories of an electron in the laser field, within a certain range of relative phase values.**

Keywords: *above-threshold ionisation of atoms, femtosecond laser pulses, numerical simulation.*

1. Introduction

The use of a two-colour laser field in the investigation of above-threshold ionisation (ATI) of atomic systems has opened up the possibility of studying a number of interesting practical applications of the effects that can be used to obtain information about the dynamics of the valence electron of an atom on the attosecond time scale [1, 2] and to control interference effects during the ATI process [2–5]. The simplest configuration of a two-colour field, i.e. two pulses with frequencies ω and 2ω, linearly polarised in the same direction, is also very effective in the generation of THz radiation [6–8]. In a recent paper [9], Skruszewicz et al. have demonstrated the possibility of extracting spectroscopic information about the atomic structure of the target from the ATI spectra in a two-colour field.

Qualitatively, the ATI process is described in the framework of the quasi-classical three-step model [10–12], which involves tunnelling ionisation of an optically active electron of the atom, its subsequent propagation in the laser field and rescattering by an ion of the parent atom with account for the additional energy gain from the laser field. Analysis of the ATI amplitude in the quasi-classical approximation shows that it can be represented as a sum of partial amplitudes associated with the classical trajectories of an electron in the laser field [12]. This approach has proven to be very productive and is now widely used for the interpretation of the experimental data and for the development of original semi-classical method for calculating the ATI spectra. One such method has been recently proposed in [5] and is based on the Monte Carlo method and the classic representation of the dynamics of an electron in the laser field. In particular, Zheng et al. [5], using the Monte Carlo method and numerical solution of the time-dependent Schrödinger equation, have studied asymmetry of the ATI spectra in a two-colour field. Despite the fairly detailed analysis of the ATI spectra in a two-colour laser field [5], a number of effects have not been considered, such as suppression of the contribution of short classical trajectories under changes in the relative phase of the field.

In this paper, we discuss the possibility of controlling the ATI process of atoms by a two-colour laser field with intensity-comparable collinear linearly polarised components. The possibility of such a control arises from the strong dependence of the position of the high-energy plateau cutoff in the ATI spectra on the relative phase of the field components in a certain range of phase values. This effect is observed numerically as a result of the solution of the time-dependent Schrödinger equation and is qualitatively explained using classical analysis of trajectories of an optical electron in a two-component field within the framework of analytic theory for ATI [13, 14].

2. ATI spectra in a two-colour laser field

In numerical calculations ATI spectra (or the momentum distribution of photoelectrons) are calculated using the wave function obtained by solving the time-dependent Schrödinger equation after the laser pulse is turned off (see, e.g., [14]):

$$P \propto \left| \int [\psi_{\boldsymbol{p}}^{(-)}(\boldsymbol{r})]^* \psi(\boldsymbol{r}, t = \tau) \mathrm{d}\boldsymbol{r} \right|^2,$$

where $\psi_{\boldsymbol{p}}^{(-)}(\boldsymbol{r})$ is the wave function from a continuous spectrum in the atomic potential $U(r)$ with the asymptotic behaviour of converging spherical waves and the asymptotic momentum $\boldsymbol{p}$; $\psi(\boldsymbol{r}, t)$ is the wave function of an electron in the laser field and the atomic potential $U(r)$; and τ is the pulse duration. The analysis shows that for the momentum distribution of high-energy electrons to be calculated, the wave function of the continuous spectrum $\psi_{\boldsymbol{p}}^{(-)}(\boldsymbol{r})$ can be replaced by a plane wave. Therefore, limiting our consideration to a high-energy part of the ATI spectrum only, we will calculate

N.V. Vvedenskii, A.N. Zheltukhin, A.A. Silaev Institute of Applied Physics, Russian Academy of Sciences, ul. Ul'yanova 46, 603950 Nizhnii Novgorod, Russia; e-mail: vved@appl.sci-nnov.ru;
D.V. Knyazeva, A.V. Flegel, M.V. Frolov Institute of Applied Physics, Russian Academy of Sciences, ul. Ul'yanova 46, 603950 Nizhnii Novgorod, Russia; Voronezh State University, Universitetskaya pl. 1, 394006 Voronezh, Russia;
N.L. Manakov Voronezh State University, Universitetskaya pl. 1, 394006 Voronezh, Russia

Received 8 February 2016
Kvantovaya Elektronika **46** (4) 361–365 (2016)
Translated by I.A. Ulitkin

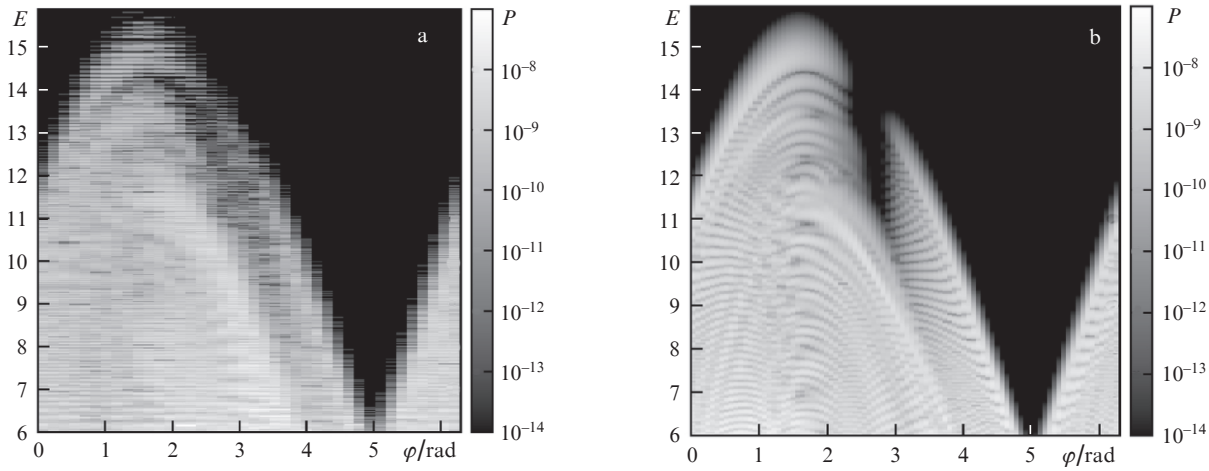

Figure 1. Dependences of the yield of high-energy electrons in the course of ATI of hydrogen atoms by a two-colour laser field on the photoelectron energy $E = p^2/2$ and the relative phase φ of the laser field components, obtained by solving numerically the time-dependent Schrödinger equation (a) and within the analytical approach [13, 14] (b). Interference effects caused by the destructive/constructive interference of short and long trajectories are clearly visible in Fig. 1b, but are not visible in Fig. 1a due to a lack of small steps in phase φ in the numerical calculations, required for the manifestation of these effects.

the momentum distribution of photoelectrons by using the relation*

$$P(\boldsymbol{p}) \propto \left| \int \exp(-\mathrm{i}\boldsymbol{p}\boldsymbol{r})\psi(\boldsymbol{r}, t = \tau)\,\mathrm{d}\boldsymbol{r} \right|^2. \quad (1)$$

The wave function of the electron at time $t = \tau$ was determined by numerical integration of the time-dependent Schrödinger equation:

$$\mathrm{i}\frac{\partial\psi(\boldsymbol{r},t)}{\partial t} = \left[-\frac{\nabla^2}{2} + U(r) + \boldsymbol{r}\boldsymbol{F}(t)\right]\psi(\boldsymbol{r},t), \quad (2)$$

where

$$\boldsymbol{F}(t) = \boldsymbol{e}_x \frac{Ff(t)}{\sqrt{1+\beta^2}}[\cos\omega t + \beta\cos(2\omega t + \varphi)]$$

is the electric field strength of a two-colour laser pulse; $f(t)$ is the pulse envelope; $\boldsymbol{e}_x$ is the unit polarisation vector of the laser field; F is the amplitude of the fundamental component of the field at a carrier frequency ω; β is the relative amplitude of the component of the second harmonic of the field; and φ is the relative phase of the field components. To reduce the effects associated with the envelope of the laser pulse, we used in the calculations a trapezoidal pulse with a two-cycle linear ramp for switching on and off and six cycles on the flat-top part of the envelope:

$$f(t) = \begin{cases} t/(2T), & 0 < t \leqslant 2T, \\ 1, & 2T < t \leqslant 8T, \\ 1 - (t - 8T)/(2T), & 8T < t \leqslant 10T, \\ 0, & t \leqslant 0,\ t > 10T, \end{cases}$$

where $T = 2\pi/\omega$. The atomic potential $U(r)$ is modelled by a smoothed Coulomb potential [15]:

$$U(r) = -\alpha\,\mathrm{sech}^2(r/a) - \tanh(r/a)/r, \quad (3)$$

where $a = 0.3$ and $\alpha = 2.17$. The choice of the parameters a and α provides coincidence of the ground-state energy of the electron in potential (3) with the ground-state energy of hydrogen, $E_\mathrm{H} = -13.6$ eV.

The time-dependent Schrödinger equation is solved by a pseudo-spectral (split-step) method using the Hankel transform and the fast Fourier transform in spatial variables [16–18]. In order to achieve the convergence of the numerical algorithm for calculating the wave function, the number of grid points along the field polarisation axis (x axis) N_x was set equal to 16384 and the number of nodes along the orthogonal direction N_ρ – to 480. Steps in time t and coordinate x were chosen as follows: $\Delta t = 0.015$, $\Delta x = 0.225$, grid nodes in the coordinate ρ (ρ is the distance to the x axis) are arranged non-equidistantly and the grid boundary corresponds to $\rho_\mathrm{max} = 74$.

Figure 1a presents numerically obtained energy distributions of photoelectrons (ATI spectra) emitted in the direction of the polarisation vector of laser radiation upon ionisation of the hydrogen atom by a two-component field at various values of the relative phase φ. The results are shown for comparable intensities of the field components ($\beta = 0.9$), main component intensity $I = cF^2/(8\pi) = 3\times10^{-3}$ ($\sim1\times10^{14}$ W cm^{-2}), its wavelength $\lambda = 2$ μm and frequency $\omega = 0.0228$ ($\sim$0.62 eV). One can see that for a wide range of energies E, the yield of photoelectrons remains on average constant, forming a so-called high-energy rescattering plateau in the ATI spectra. The position of the region of the plateau cutoff (behind which the ATI yield is sharply reduced) is described mostly by a smooth harmonic dependence on the phase φ, except for the interval $\varphi \approx 2.4$–3 rad, for which there is a dip in the spectrum of photoelectrons. For this range of the phase shift of the second harmonic of the field, the maximum energy of photoelectrons in the plateau region is significantly reduced. Numerical analysis shows that at comparable intensities of the frequency components of the laser field, the dip of the spectrum of the ATI yield disappears and a harmonic dependence of the position of the plateau cutoff on φ holds for the entire range of φ values.

* Hereafter we use atomic units.

3. Interpretation of numerical results

For a qualitative explanation of the sharp suppression of the yield of high-energy electrons by varying the relative phase of the two-colour field, we use an analytical approach to the description of the high-energy part of the ATI spectrum [13, 14]. Briefly, in this approach, the ATI amplitude of high-energy electrons $A^{\mathrm{R}}(\boldsymbol{p})$ can be represented as the sum of the partial amplitudes A_j:

$$A^{\mathrm{R}}(\boldsymbol{p}) = \sqrt{\mathrm{i}}\,\omega \sum_j A_j . \tag{4}$$

Each of the amplitudes A_j is associated with times $t_{\mathrm{i}}^{(j)}$ and $t_{\mathrm{f}}^{(j)}$, having the sense of the initial (subscript i) and final (subscript f) moments of time during the electron motion along the jth closed classical trajectory under the action of the laser field. These times may can be obtained from the analysis of saddle-point equations in the approximate calculation of the integral for the amplitude $A^{\mathrm{R}}(\boldsymbol{p})$ by the saddle-point method and are determined by a system of equations [11, 13, 14]

$$A(t_{\mathrm{i}}^{(j)}) - \frac{1}{t_{\mathrm{f}}^{(j)} - t_{\mathrm{i}}^{(j)}} \int_{t_{\mathrm{i}}^{(j)}}^{t_{\mathrm{f}}^{(j)}} A(\tau)\,\mathrm{d}\tau = 0, \tag{5a}$$

$$2F(t_{\mathrm{f}}^{(j)}) + \frac{1}{c}\frac{A(t_{\mathrm{f}}^{(j)}) - A(t_{\mathrm{i}}^{(j)})}{t_{\mathrm{f}}^{(j)} - t_{\mathrm{i}}^{(j)}} = 0, \tag{5b}$$

where $F(t) = \boldsymbol{e}_x \boldsymbol{F}(t)$; $A(t) = \boldsymbol{e}_x \boldsymbol{A}(t)$; and $\boldsymbol{A}(t)$ is the vector potential of the laser field [$\boldsymbol{F}(t) = -c^{-1}\dot{\boldsymbol{A}}(t)$]. Equations (5a) and (5b) have a simple classical interpretation. Equation (5a) shows that at the time of ionisation, $t = t_{\mathrm{i}}^{(j)}$, the electron leaves the atomic system with zero velocity and moves in a laser field along a closed trajectory up to time $t_{\mathrm{f}}^{(j)}$. At the time of return, $t = t_{\mathrm{f}}^{(j)}$, the electron is backscattered by the atomic core, and equation (5b) implies that the electron has a maximum energy after such backscattering.

Classical trajectories associated with times $t_{\mathrm{i}}^{(j)}$ and $t_{\mathrm{f}}^{(j)}$ can be classified as single-return and multiple-return in accordance with the number of returns of the electron to the atomic core during the time $\Delta t_j = t_{\mathrm{f}}^{(j)} - t_{\mathrm{i}}^{(j)}$ between the moments of ionisation and rescattering. Single-return trajectories imply that the electron moves along these trajectories and during the time Δt_j returns once to the atomic core and experiences rescattering. Moving along multiple-return trajectories, the electron returns to the atomic core several times before being rescattered. Because the times $t_{\mathrm{i}}^{(j)}$ and $t_{\mathrm{f}}^{(j)}$ depend on the relative phase φ, the change in the latter allows the times of ionisation and rescattering to be controlled. As a rule, the main contribution to the formation of the high-energy part of the ATI spectrum is made by a single-return trajectory with a minimum return time $\Delta t_j < 2\pi/\omega$, because for these trajectories the kinetic energy gained by the electron as a result of its movement along a closed trajectory is maximum by the time of rescattering. The energy gained by the electron moving along a closed trajectory is approximately determined by the square of the difference of vector potentials at the times $t = t_{\mathrm{i}}^{(j)}$ and $t = t_{\mathrm{f}}^{(j)}$ [13, 14]:

$$E_{\max}^{(j)} = \frac{1}{2}\left[A(t_{\mathrm{i}}^{(j)}) - A(t_{\mathrm{f}}^{(j)})\right]^2 - 2\,|E_0|\,\frac{F(t_{\mathrm{f}}^{(j)})}{F(t_{\mathrm{i}}^{(j)})} =$$

$$\approx \frac{1}{2}\left[A(t_{\mathrm{i}}^{(j)}) - A(t_{\mathrm{f}}^{(j)})\right]^2, \tag{6}$$

where the second term, proportional to the bound state energy E_0, yields a small quantum correction to the classical result. It can be shown [12, 14] that $E_{\max}^{(j)}$ takes the highest values for those trajectories, the beginning and the end of the movement along which are in the vicinity of the extrema of the laser field strength and vector potential, respectively. It should also be noted that multiple-return trajectories make a substantial contribution to the middle part of the high-energy plateau and do not affect the part of the ATI spectrum near the top boundary of the plateau [14].

The partial amplitude A_j, which determines the amplitude (4), is represented as a product of three factors describing the three-step scenario of the ATI process [10]:

$$A_j = a_\tau^{(j)} a_W^{(j)} a_{\mathrm{s}}^{(j)} \exp(\mathrm{i}S_j). \tag{7}$$

The factor $a_\tau^{(j)}$ describes tunnelling of the electron from an atom in the first stage of the scenario. Motion of the electron in the laser field along a closed trajectory in the second stage is determined by the factor $a_W^{(j)}$, and the subsequent rescattering on the atomic core is described by the amplitude $a_{\mathrm{s}}^{(j)}$ of elastic scattering of the electrons by the ion of the parent atom. The value of S_j determines the classical action of the electron, corresponding to the movement along a closed trajectory, starting and ending at $t_{\mathrm{i}}^{(j)}$ and $t_{\mathrm{f}}^{(j)}$, respectively. Following the analytical model proposed in [13, 14], the factor $a_\tau^{(j)}$ is determined by the tunnelling ionisation probability Γ_{st} in a constant electric field with an effective strength $\tilde{F}_j = |F(t_{\mathrm{i}}^{(j)})|$ [19]:

$$a_\tau^{(j)} \propto \sqrt{\Gamma_{\mathrm{st}}(\tilde{F}_j)}, \tag{8}$$

and the propagation factor $a_W^{(j)}$ is expressed in terms of the Airy function $\mathrm{Ai}(x)$:

$$a_W^{(j)} \propto \mathrm{Ai}[\alpha_j(E_j - E_{\max}^{(j)})],$$

$$E_j = \frac{1}{2}\left[\boldsymbol{p} + \frac{1}{c}\boldsymbol{A}(t_f^{(j)})\right]^2, \tag{9}$$

where $\boldsymbol{p}$ is the momentum of the photoelectron, and the parameter α_j is expressed in terms of the electric field strength at times $t_{\mathrm{i}}^{(j)}$ and $t_{\mathrm{f}}^{(j)}$ [13, 14]. The amplitude of elastic scattering $a_{\mathrm{s}}^{(j)}$ in (7) describes the elastic scattering of the electron (rescattering) by the atomic core with the initial ($\boldsymbol{p}_{\mathrm{i}}$) and final ($\boldsymbol{p}_{\mathrm{f}}$) momenta $\boldsymbol{p}_{\mathrm{i}}^{(j)} = \boldsymbol{e}_x |\boldsymbol{P}_j|$ and $\boldsymbol{p}_{\mathrm{f}}^{(j)} = \boldsymbol{P}_j$, where $\boldsymbol{P}_j = \boldsymbol{p} + c^{-1}\boldsymbol{A}(t_{\mathrm{f}}^{(j)})$.

The explicit expression (7) for the partial ATI amplitude points to possible ways of suppressing or enhancing certain partial amplitudes. Indeed, a change in the time dependence of the field, for example by varying the relative phase in the case of a two-colour-field, causes a significant change (due to the exponential dependence of Γ_{st} on the laser field strength) in the factor $a_\tau^{(j)}$. An increase (decrease) in the factor $a_\tau^{(j)}$ leads to a predominance (suppression) of a particular term in sum (4). As will be shown below, in the case of a two-colour field the phase variation causes suppression of a whole group of partial amplitudes.

Consider the time dependence of the two-colour laser field with comparable intensities of the components shown in Fig. 2. During a cycle of the main components $T = 2\pi/\omega$, the laser field has four extrema corresponding to two local maxima and minima. In one of the two minima located in the vicinity of the half-cycle, the field strength is maximum in absolute value, and therefore, the ionisation factors of the partial amplitudes corresponding to the classical trajectories with $t_i^{(j)} \approx (j + 1/2)T$ ($j = 0, 1, 2, ...$) will be greatest. However, these trajectories exhibit multiple-return behaviour (see the lower graph in Fig. 2) and contribute to the middle part of the high-energy plateau. The value of the electric field in the vicinity of the second minimum is close to zero, and the partial amplitudes corresponding to the classical trajectories with $t_i^{(j)} \approx jT$ will be suppressed due to a significant decrease in the tunnelling ionisation probability, which determines the factor $a_\tau^{(j)}$. One can see from Fig. 2 that also possible is the suppression of the contribution from the single-return trajectory that defines the boundary of the high-energy plateau. Thus, in suppressing the contribution of the short trajectory, the boundary of the high-energy plateau is defined by the multiple-return trajectory, which leads to a decrease in energy, which determines the region of the plateau cutoff.

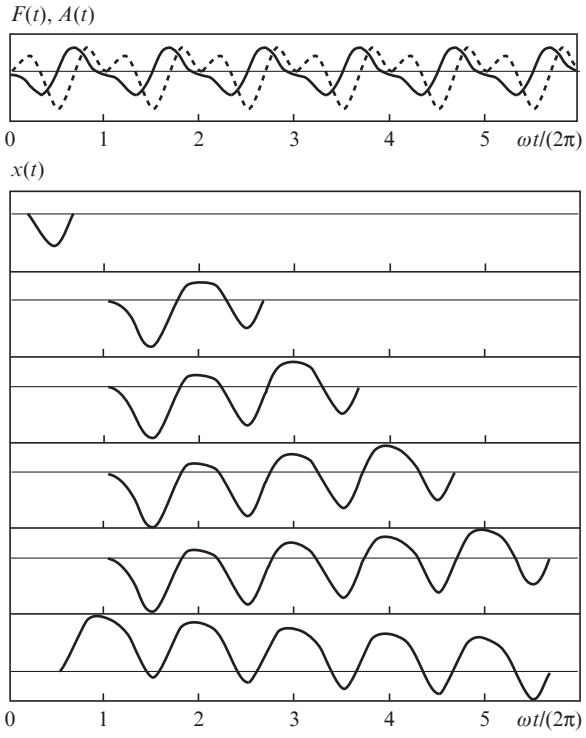

Figure 2. Time dependences of the strength (dashed curve) and vector potential (solid vurve) of a two-colour field with $\beta = 0.9$ and $\varphi = 2.8$ rad (top figure), as well as the laws of motion of the electron along single- and multiple-return closed classical trajectories.

Analysing the ionisation factor as the relative phase of the field function for different numbers $a_\tau^{(j)}$ of classical trajectories, we have found that in the interval $\varphi \in (2.4 \text{ rad}, 2.6 \text{ rad})$ the single-return trajectory ($j = 1$) is suppressed with a minimal time Δt_1 of electron motion along a closed trajectory and the highest energy of the electron $E_{cut}^{(1)}$ after rescattering (for $\varphi = 2.4$ rad we have $\omega\Delta t_1 = 4.49$, $E_{cut}^{(1)} = 15.32u_p$, $u_p = [F^2/(4\omega^2)]\{1 - 3\beta^2/[4(1 + \beta^2)]\}$). In this case, the length of the plateau in the ATI spectrum is determined by the trajectory ($j = 2$) with a great time $\Delta t_2 > \Delta t_1$ and a lower energy $E_{cut}^{(2)} < E_{cut}^{(1)}$. With a further increase in φ, the following [in order of decreasing energy $E_{cut}^{(j)}$] partial ATI amplitudes A_j [and correspondingly $\Gamma_{st}(\tilde{F}_j)$] are suppressed. Thus, at $\varphi = 2.8$ rad suppressed are four multiple-return trajectories, as a result of which the plateau length is determined by the trajectory with $\omega\Delta t_5 = 29.81$ and $E_{cut}^{(5)} = 12.11u_p$.

Outside the phase interval from 2.35 to 2.85 rad, the form of the high-energy plateau, as well as the position of the region of its cutoff can be estimated with high accuracy in the framework of the approximation of single-return trajectories (as in the case of a monochromatic field and a short laser pulse). Thus, by varying the relative phase and amplitude of the second harmonic component of the two-colour field [leading to a decrease in the effective value of the laser field in the first step (tunnelling) of the three-step ATI scenario], one can suppress some partial ionisation amplitudes determining the yield of high-energy photoelectrons.

It should be noted that despite good qualitative agreement of the ATI spectra obtained from the solution of the time-dependent Schrödinger equation and calculated on the basis of the analytic theory [13, 14], there is a significant quantitative difference between the two results (see., e.g., the photoelectron yield in Fig. 1 for $\varphi \in (2.4 \text{ rad}, 2.6 \text{ rad})$. The emergence of this difference is due to the restrictions imposed on the parameters of the laser field in the construction of the analytic theory [13, 14]. In fact, one of the key assumptions of the theory [13, 14] is the smallness of the Keldysh parameter γ_j at the ionisation time $t_i^{(j)}$: $\gamma_j = \sqrt{2|E_0|}\,\omega/\tilde{F}_j \ll 1$. It is obvious that this assumption allows us to express the ionisation factor $a_\tau^{(j)}$ through the tunnelling probability in the effective constant electric field [see relation (8)]. However, in the region of suppression of single-return trajectories the Keldysh parameter becomes the order of unity (because of the smallness of the absolute value of the field strength) and the value of the ionisation factor, given by the analytical theory, is significantly underestimated in comparison with the real one. This is due to the fact that a decrease in the ionisation rate with a decrease in the electric field amplitude (i.e. with an increase in the Keldysh parameter) in the tunnelling limit occurs much more rapidly (exponentially) than in the multiphoton case (when the Keldysh parameter becomes greater than or of the order of unity, and the ionisation rate decreases with decreasing electric field amplitude in accordance with the power law). The underestimated value of the ionisation factor in the analytic theory causes a sharper dip in the spectrum of the photoelectron yield in Fig. 1b as compared with the numerical results shown in Fig. 1a for the phases $\varphi \in (2.4 \text{ rad}, 2.6 \text{ rad})$.

4. Conclusions

We have analysed the ATI spectra of atoms in an intense, two-colour laser field with collinear linearly polarised components. Using the numerical solution of the time-dependent Schrödinger equation, we have found that for comparable intensities of the frequency components of the laser pulse (with centre frequencies ω and 2ω) the boundary of the high-energy plateaus in the ATI spectra is substantially modified under changes in the relative phase φ of the field components. This modification takes the form of a marked dip in the spectrum of high-energy photoelectrons in a narrow range of φ values, resulting in a sharp decrease in the plateau length.

To analyse and interpret the above numerical results, we have used the analytical theory for ATI [13, 14], modified for the case of a two-colour field. As part of this analytical approach, the ATI amplitude is represented as a coherent sum of partial amplitudes, each of which is associated with a closed 'extreme' trajectory ensuring a maximum photoelectron energy after rescattering by the atomic core. Considering 'extreme' trajectories as single-return and multiple-return ones and exploring their properties, we have presented a physically transparent quasi-classical interpretation of the obtained numerical dip in high-energy photoelectron spectrum: partial ionisation amplitudes associated with the shortest trajectories corresponding to the maximum permissible classical electron energy at the moment of rescattering are suppressed at certain values of the relative phase φ and comparable intensities of the field component. This suppression is caused by the suppression of the channel of tunnelling ionisation due to a decrease in the effective field at the time of ionisation, determining the ionisation factor in the framework of the three-step scenario of formation of the high-energy plateau in the ATI spectra. Finally, the presented mechanism of suppression of the contribution of individual trajectories into the ATI spectra enables in principle the control of the ATI process of the atoms by varying the two-colour laser field parameters: the ratio of the amplitudes and relative phase of its components.

Acknowledgements. This work was supported by the Russian Scientific Foundation (Grant No. 15-12-10033).

References

1. Xie X., Roither S., Kartashov D., Persson E., Arbó D.G., Zhang L., Gräfe L., Schöffler M.S., Burgdörfer J., Baltuška A., et al. *Phys. Rev. Lett*., **108**, 193004 (2012).
2. Arbó D.G., Nagele S., Tong X.-M., Xie X., Kitzler M., Burgdörfer J. *Phys. Rev. A*, **89**, 043414 (2014).
3. Arbó D.G. *J. Phys. B*, **47**, 204008 (2014).
4. Arbó D.G., Lemell C., Nagele S., Camus N., Fechner L., Krupp A., Pfeifer T., López S.D., Moshammer R., Burgdörfer J. *Phys. Rev. A*, **92**, 023402 (2015).
5. Zheng X., Liu M.-M., Xie H., Ge P., Li M., Liu Y. *Phys. Rev. A*, **92**, 053422 (2015).
6. Babushkin I., Kuehn W., Köhler C., Skupin S., Bergé L., Reimann K., Woerner M., Herrmann J., Elsaesser T. *Phys. Rev. Lett*., **105**, 053903 (2010).
7. Vvedenskii N.V., Korytin A.I., Kostin V.A., Murzanev A.A., Silaev A.A., Stepanov A.N. *Phys. Rev. Lett*., **112**, 055004 (2014).
8. Popruzhenko S.V., Tulsky V.A. *Phys. Rev. A*, **92**, 033414 (2015).
9. Skruszewicz S., Tiggesbäumker J., Meiwes-Broer K.-H., Arbeiter M., Fennel Th., Bauer D. *Phys. Rev. Lett.*, **115**, 043001 (2015).
10. Paulus G.G., Becker W., Nicklich W., Walther H. *J. Phys. B*, **27**, L703 (1994).
11. Becker W., Grasbon F., Kopold R., Milošević D.B., Paulus G.G., Walther H. *Adv. At. Mol. Opt. Phys*., **48**, 35 (2002).
12. Milošević D.B., Paulus G.G., Bauer D., Becker W. *J. Phys. B*, **39**, R203 (2006).
13. Frolov M.V., Knyazeva D.V., Manakov N.L., Popov A.M., Tikhonova O.V., Volkova E.A., Xu M.-H., Peng L.-Y., Pi L.-W., Starace A.F. *Phys. Rev. Lett*., **108**, 213002 (2012).
14. Frolov M.V., Knyazeva D.V., Manakov N.L., Geng J.-W., Peng L.-Y., Starace A.F. *Phys. Rev. A*, **89**, 063419 (2014).
15. Gordon A., Kärtner F.X. *Phys. Rev. Lett*., **95**, 223901 (2005).
16. Silaev A.A., Vvedenskii N.V. *Phys. Rev. Lett*., **102**, 115005 (2009).
17. Silaev A.A., Ryabikin M.Yu., Vvedenskii N.V. *Phys. Rev. A*, **82**, 033416 (2010).
18. Silaev A.A., Vvedenskii N.V. *Phys. Plasmas*, **22**, 053103 (2015).
19. Smirnov B.M., Chibisov M.I. *Zh. Eksp. Teor. Fiz*., **49**, 841 (1965).